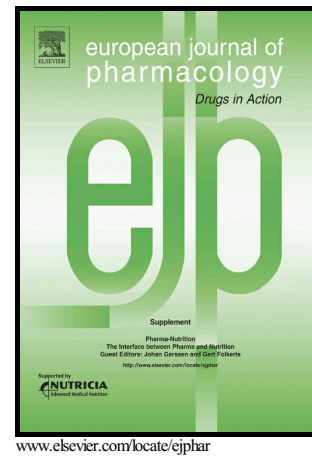


Author's Accepted Manuscript

Protective effects of VGX-1027 in PM_{2.5}-induced airway inflammation and bronchial hyperresponsiveness

Mengmeng Xu, Feng Li, Muyun Wang, Hai Zhang, Lu Xu, Ian M. Adcock, Kian Fan Chung, Yanbei Zhang



PII: S0014-2999(18)30658-7
DOI: <https://doi.org/10.1016/j.ejphar.2018.11.010>
Reference: EJP72072

To appear in: *European Journal of Pharmacology*

Received date: 4 October 2018
Revised date: 7 November 2018
Accepted date: 7 November 2018

Cite this article as: Mengmeng Xu, Feng Li, Muyun Wang, Hai Zhang, Lu Xu, Ian M. Adcock, Kian Fan Chung and Yanbei Zhang, Protective effects of VGX-1027 in PM_{2.5}-induced airway inflammation and bronchial hyperresponsiveness, *European Journal of Pharmacology*, <https://doi.org/10.1016/j.ejphar.2018.11.010>

This is a PDF file of an unedited manuscript that has been accepted for publication. As a service to our customers we are providing this early version of the manuscript. The manuscript will undergo copyediting, typesetting, and review of the resulting galley proof before it is published in its final citable form. Please note that during the production process errors may be discovered which could affect the content, and all legal disclaimers that apply to the journal pertain.

Protective effects of VGX-1027 in PM_{2.5}-induced airway inflammation and bronchial hyperresponsiveness

Mengmeng Xu^{a1}, Feng Li^{b1}, Muyun Wang^a, Hai Zhang^b, Lu Xu^a, Ian M Adcock^c, Kian Fan Chung^c, Yanbei Zhang^{a*}

^aDepartment of Respiratory and Critical Care Medicine, The Geriatric Institute of Anhui, The First Affiliated Hospital of Anhui Medical University, Hefei, Anhui, PR China 230032

^bDepartment of Pulmonary Medicine, Shanghai Chest Hospital, Shanghai Jiao Tong University, Shanghai, PR China 200030

^cAirway Disease Section, National Heart and Lung Institute, Imperial College London, London, SW3 6LY, UK

***Corresponding author.** Professor Yanbei Zhang Department of Respiratory and Critical Care Medicine, The Geriatric Institute of Anhui, The First Affiliated Hospital of Anhui Medical University, Hefei, Anhui, PR China 230032 Tel.: 0086-13805512430. zhangyanbei1963@126.com

¹ These authors contributed equally to this work.

ABSTRACT

Fine particulate matter (PM_{2.5}) can penetrate into alveolar spaces and induce airway inflammation. Recent evidence suggests that the activation of Toll-like receptor 4 (TLR4) signaling may participate in PM_{2.5}-induced acute lung injury. We investigated the effect of VGX-1027, a TLR4 blocker, on PM_{2.5}-induced airway inflammation and bronchial hyperresponsiveness (BHR) in a murine model *in vivo* and on inflammatory mechanisms *in vitro* in human airway epithelial cells. Mice were injected intraperitoneally with vehicle (PBS) or VGX-1027 (25 mg/kg) one hour before intranasal instillation of vehicle (PBS) or PM_{2.5} (7.8 mg/kg) for two consecutive days and inflammatory events and BHR studied 24 h later. Human airway epithelial Beas-2b cells were pretreated with vehicle or VGX-1027 (50 μM) *in vitro* one hour before incubation with vehicle or PM_{2.5} (150 ng/ml) for 24 h and effects on inflammatory mediators and mechanisms studied. VGX-1027 pretreatment attenuated PM_{2.5}-induced BHR and elevated total and neutrophils, macrophages, lymphocytes and eosinophils numbers in bronchoalveolar lavage (BAL) fluid *in vivo*. PM_{2.5}-induced BAL fluid inflammatory mediator levels including TNF-α, chemokine (C-X-C motif) ligand1, IL-1β, IL-6 and IL-18 were reduced by VGX-1027. PM_{2.5}-induced increases in TNF-α, IL-1β, IL-6 and IL-18 mRNA levels in Beas-2b cells were also reduced by VGX-1027. Mechanistically, VGX-1027 inhibited PM_{2.5}-induced activation of the TLR4-NF-κB-p38 MAPK and NLRP3-caspase-1 pathways as well as the dysregulation of mitochondrial fusion/fission proteins *in vivo* and *in vitro*. VGX-1027 may be a potential prophylactic treatment for PM_{2.5}-induced acute lung injury that has airway inflammation, BHR and mitochondrial damage.

Keywords: fine particulate matters (PM_{2.5}); airway inflammation; bronchial hyperresponsiveness; VGX-1027; toll-like receptor 4; mitochondrial damage

1. Introduction

Air pollution has become increasingly severe in China in recent years due to rapid industrialization and urbanization. Fine particulate matter (aerodynamic diameter <2.5 μm), known as PM_{2.5}, contains abundant substances harmful to the human body (Lin et al., 2018). PM_{2.5} pollution is significantly associated with the increasing morbidity and mortality of various respiratory diseases, such as asthma, chronic obstructive pulmonary disease (COPD) and lung carcinoma (Xing et al., 2016). PM_{2.5} can be inhaled and deposited in the lung, penetrate into the alveolar space and even enter into the circulation. This results in pulmonary and systemic inflammation and immune responses.

Acute PM_{2.5} exposure induces bronchial hyperresponsiveness (BHR), airway inflammation with the release of proinflammatory cytokines and chemokines, and mitochondrial damage (Guo et al., 2017; Ogino et al., 2017). PM_{2.5} can directly act on mitochondrial membranes to cause the disruption of mitochondrial structure and function together with alteration in expression of mitochondrial fusion/fission proteins (Guo et al., 2017; Li et al., 2015b; Ovreik et al., 2015). Moreover, PM_{2.5}-induced mitochondrial damage may also lead to the activation of innate immune responses (Miyata and van Eeden, 2011).

As one of innate immunity pathways, Toll-like receptor 4 (TLR4) signaling, along with

myeloid differentiation primary response 88 (MyD88), promotes the polyubiquitination of TNF receptor associated factor 6 (TRAF6), which then drives the activation of nuclear factor-kappa B (NF- κ B) and mitogen-activated protein kinases (MAPKs) and the subsequent induction of proinflammatory gene expression (Kawasaki and Kawai, 2014). Some studies have reported that the activation of TLR4 pathway may be involved in PM_{2.5}-induced murine airway/lung inflammation (He et al., 2017; Wang et al., 2017). In TLR4^{-/-} mice, the pro-inflammatory actions of PM_{2.5} was decreased as was airway inflammation (He et al., 2017). The nucleotide binding domain leucine-rich repeat-containing receptor (NLR) family, of which NLRP3 is the most widely characterized member, are also important innate immunity pathways. The activation of NLRP3 can initiate the release of proinflammatory cytokines such as IL-1 β and IL-18 (Sandhir et al., 2017).

VGX-1027, also known as GIT27, is an isoxazoline compound [(S, R)-3-phenyl-4, 5-dihydro-5-isoxasole acetic acid] and a potent immunomodulator (Cha et al., 2013; Stojanovic et al., 2007). VGX-1027 inhibits LPS-induced synthesis of TNF- α , IL-1 β and IL-10 from mouse peritoneal macrophages and reduced TNF- α synthesis from mouse spleen mononuclear cells (Stojanovic et al., 2007). VGX-1027 also inhibited high glucose- and high free fatty acid-induced TNF- α , IL-1 α and IL-4 levels in mouse podocytes and adipocytes and decreased TLR4-mediated IL-2 and TNF- α expression in an experimental mouse model of diabetes (Cha et al., 2013). Moreover, VGX-1027 modulated inflammatory gene expression following LPS stimulation in human peripheral blood mononuclear cells (Fagone et al., 2014).

Up to now, the protective effects of VGX-1027 on acute airway inflammation and BHR has not been elucidated and there have been no studies on whether VGX-1027 can inhibit PM_{2.5}-induced acute airway inflammation and BHR. In present study, we evaluated the protective effect of VGX-1027 on PM_{2.5}-induced airway inflammation and BHR. We also analyzed the potential mechanisms that may be involved in the anti-inflammatory effect of VGX-1027 *in vivo* and using a human airway epithelial Beas-2b cell line.

2. Materials and Methods

2.1. PM_{2.5} sampling and extraction

PM_{2.5} samples were collected by a Medium Flow PM_{2.5} Sampler (Laoying Model 2030, China) from August 2016 to June 2017. The PM_{2.5} Sampler was located on the top of a building in a non-industrial block in Shanghai, China. The sampler removed particles that were greater than 2.5 μm and collected the remaining particles (the PM_{2.5} fraction) on a Glass Fiber Filter. PM_{2.5} fiber filters were sheared into smaller fragments, immersed into ultrapure water and eluted with an ultrasonic cleaner, followed by freezing and vacuum drying. Finally, PM_{2.5} solid particulates were collected and preserved in the -20°C freezer. Before the experiment, quantitative PM_{2.5} solid particulates were evenly suspended in phosphate buffer saline (PBS) by vortexing and stored at 4°C.

2.2. Mice, PM_{2.5} instillation and VGX-1027 administration

Thirty two 8-week-old male C57/BL6 mice, weight 22-25 g, were provided by Shanghai Super--B&K Laboratory Animal Corporation (Shanghai, China). All the mice were fed with standard diet in specific pathogen-free housing at 22°C with 50-60% humidity and an

equal light-dark cycle. All experimental studies involving animals were approved by the laboratory animal ethics committee of the institute. Mice were injected intraperitoneally with vehicle (PBS) or VGX-1027 (25 mg/kg dissolved in 2% DMSO/ 30% PEG400/ 5% Tween, Selleck, Houston, TX, USA). One hour later, the mice inhaled isoflurane before being instilled intranasally with PBS or PM_{2.5} particulates (7.8 mg/kg) suspended in 50 µl of PBS for two consecutive days. The mice were studied 24 h later.

2.3. Cell culture, PM_{2.5} incubation and VGX-1027 administration

Beas-2b cells, a human bronchial epithelial cell (obtained from Shanghai Institutes for Biological Sciences, China Academy of Science, Shanghai) were cultured in 1640 Medium (Hyclone, Logan, UT, USA) with 10% fetal bovine serum (Biolnd, Kibbutz Beit Haemek, Israel), 100 U/ml penicillin and 100 µg/ml streptomycin (Thermo-Fisher Scientific, Waltham, MA, USA) at 37°C under saturated humidity and 5% CO₂. When grown to 70% confluence, the medium was refreshed with new media containing vehicle (PBS) or VGX-1027 (50 µM, Selleck) and incubated for 60 min. Then, cells were incubated with the vehicle/PM_{2.5} suspension (150 ng/ml) for 24 h.

2.4. BHR measurement

After anesthesia with an intraperitoneal injection of 0.2 ml 1% pentobarbital, mice were tracheostomized and placed in a whole-body plethysmograph for the measurement of resistance and compliance (EMMS, Hants, UK). The concentration of acetylcholine (ACh) required to increase lung resistance by 200% from baseline was calculated (PC₂₀₀), and -logPC₂₀₀ was taken as a measure of bronchial responsiveness.

2.5. Bronchoalveolar lavage (BAL) fluid collection, cell counting and cytokine assay

Following terminal anaesthesia with pentobarbitone, mice were lavaged with 2 ml aliquots of PBS via an endotracheal tube. The bronchoalveolar lavage (BAL) fluid was centrifuged at 4°C, 92 g for 10 min, cell pellets were re-suspended in PBS. Total cell counts were determined using a hemocytometer, and differential cell counts from cytopsin preparations stained by Liu's stain solution (Baso Diagnostics Inc, Zhuhai, China) were measured under a microscope. At least 500 cells were counted and identified as macrophages, lymphocytes, neutrophils and eosinophils.

The levels of TNF- α , chemokine (C-X-C motif) ligand 1 (KC), IL-1 β , IL-6 and IL-18 in BAL fluid were measured with specific ELISA kits (Mutisciences, Hangzhou, China) following the Manufacturer's instructions.

2.6. Histology and immunohistochemistry of TLR4

The whole lung was removed from the chest and the right lung lobes were dissected and snap frozen in liquid nitrogen for later analysis. The left lung was inflated with 4% paraformaldehyde under 25 cm of water pressure and then embedded in paraffin. Paraffin blocks were sectioned to expose the maximum surface area of lung tissue in the plane of the bronchial tree. Four μm sections were cut and stained with haematoxylin and eosin (H&E) for evaluating the extent of lung inflammation, and the scores were measured on a scale of 0-3 as previously described (Li et al., 2013).

Immunohistochemical staining was performed to characterize the localization and expression of TLR4 (Abcam, Cambridge, MA, USA). Lung sections were incubated with anti-Toll-like receptor 4 (TLR4) primary antibody (Abcam, USA), horseradish peroxidase (HRP)-conjugated secondary antibody followed by diaminobenzidine (DAB) liquid. The

intensity of TLR4 immunostaining was scored as described previously (Li et al., 2013).

2.7. Caspase-1 activity assay

Caspase-1 activity in lung tissue and Beas-2b cells was detected using a Caspase-1 Activity Assay Kit (Beyotime Biotechnology, Haimen, Jiangsu, China). Mouse lung tissues or Beas-2b cells were homogenized before centrifugation at 20627 g/min for 15 min at 4°C. The supernatants were transferred to pre-cooled centrifuge tubes, and caspase-1 activity was determined immediately. In brief, the substrate, Ac-YVAD-pNA, was added to the supernatant and incubated for 60-120 min at 37°C. When the solution showed an obvious yellow pNA colour, the reaction was stopped and the sample assayed by Varioskan Flash (Thermo-Fisher Scientific) at 405 nm. The level of caspase-1 activity was quantified using a standard curve.

2.8. Isolation of mRNA and gene expression

Total mRNA was extracted from cells using TRIzol reagent (TaKaRa, Dalian, Liaoning, China). The concentration of the total RNA was determined using an ultraviolet spectrophotometer. Reverse transcription (RT) was performed using a Prime Script™ RT Master Mix Kit (TaKaRa) according to the Manufacturer's instructions. RT-PCR was performed using a Power Green qPCR Mix (TaKaRa) and an ABI ViiATM 7 System. The specific primers for β -actin, TNF- α , IL-1 β , IL-6 and IL-18 were generated by BioTNT (Shanghai, China), and with the primer sequences: TNF- α , forward: 5'-TGGGATCATTGCCCTGTGAG -3', reverse: 5'-GGTGTCTGAAGGAGGGGGTA -3'; IL-1 β , forward: 5'-ATGATGGCTTATTACAGTGGCAA -3', reverse: 5'-GTCGGAGATTCGTAGCTGGA -3'; IL-6, forward: 5'-ACTCACCTCTTCAGAACGAATTG

-3', reverse: 5'- CCATCTTTGGAAGGTTTCAGGTTG -3'; IL-18, forward: 5'-
TCTTCATTGACCAAGGAAATCGG -3', reverse: 5'- TCCGGGGTGCATTATCTCTAC -3';
 β -actin, forward: 5'- GTACGCCAACACAGTGCTGTC-3', reverse: 5'-
GCTCAGGAGGAGCAATGATCTTG -3'. All samples were assayed in triplicate, and the
values were normalized to β -actin.

2.9. Western blot analysis

Total proteins were extracted from mouse lung tissues or Beas-2b cells with RIPA lysis
buffer (Beyotime Biotechnology, China), and protein concentrations were quantified by
Pierce BCA assay kit (Thermo-Fisher Scientific). 30 μ g protein per lane were separated in
10–15% denaturing polyacrylamide gels and transferred to PVDF membranes. The
membranes were blocked with 5% nonfat dry milk and incubated with the following
primary antibodies: Mitofusion-2 (MFN2), Optic Atrophy 1 (OPA1), Mitochondrial fission
factor (MFF), Dynamin-related protein 1 (Drp1), phosphorylated (phospho) NF- κ B P65,
total NF- κ B P65, phosphorylated (phospho) p38 MAPK, total p38 MAPK and NLRP3
antibodies (all from Cell Signaling Technology, Danvers, MA, USA) and with TLR4 and
Caspase-1 antibodies (Abcam, USA) overnight at 4°C. The membranes were
subsequently incubated with an HRP-conjugated anti-rabbit secondary antibody (Cell
Signaling Technology), and visualized by chemiluminescence.

2.10. Statistical analysis

All results were presented as mean \pm S.E.M. Statistical analysis was performed using
GraphPad Prism 5.0c (GraphPad Software, Inc., San Diego, CA). Two-way ANOVA was
performed for comparisons of % change in lung resistance between individual groups.

One-way ANOVA with Bonferroni's post hoc test (for equal variance) or Dunnett's T3 post hoc test (for unequal variance) was performed for comparisons among multiple groups. $P < 0.05$ was considered statistically significant.

3. Results

3.1. BHR

PBS-pretreated PM_{2.5}-instilled mice demonstrated a left ward shift of the concentration–response curve (**Fig. 1A**) with an elevated airway resistance (5.29 ± 0.19 versus 3.49 ± 0.16 , $P < 0.001$, **Fig. 1B**) and a decrease in $-\log PC_{200}$ indicating an increase in bronchial responsiveness to ACh compared to PBS-pretreated PBS-instilled mice ($-\log PC_{200}$: 1.55 ± 0.05 versus 2.09 ± 0.08 , $P < 0.001$, **Fig. 1C**). VGX-1027 pretreatment did not change basal bronchial responsiveness to ACh in PBS-instilled mice compared to PBS-pretreated PBS-instilled mice. However, VGX-1027 pretreatment decreased airway resistance (3.56 ± 0.34 versus 5.29 ± 0.19 , $P < 0.01$, **Fig. 1B**) and inhibited BHR (1.93 ± 0.13 versus 1.55 ± 0.05 , $P < 0.05$, **Fig. 1C**) in PM_{2.5}-instilled mice compared to PBS-pretreated PM_{2.5}-instilled mice.

3.2. BAL fluid cells

PBS-pretreated PM_{2.5}-instilled mice demonstrated significant increases in total cell counts (486.875 ± 27.074 vs 187.500 ± 12.320 , $P < 0.001$, **Fig. 2A**); including macrophages (250.065 ± 13.457 vs 162.002 ± 10.394 , $P < 0.001$, **Fig. 2B**), lymphocytes (64.824 ± 4.127 vs 19.198 ± 1.749 , $P < 0.001$, **Fig. 2C**), neutrophils (174.827 ± 10.988 vs 3.836 ± 0.590 , $P < 0.001$, **Fig. 2D**) and eosinophils (9.659 ± 0.716 vs 2.463 ± 0.355 , $P < 0.001$, **Fig. 2E**) in BAL fluid

compared with PBS-pretreated PBS-instilled mice (486.875 ± 27.074 vs 187.500 ± 12.320 , $P < 0.001$ [Fig. 2A]; 250.065 ± 13.457 vs 162.002 ± 10.394 , $P < 0.001$ [Fig. 2B]; 64.824 ± 4.127 vs 19.198 ± 1.749 , $P < 0.001$ [Fig. 2C]; 174.827 ± 10.988 vs 3.836 ± 0.590 , $P < 0.001$ [Fig. 2D]; 9.659 ± 0.716 vs 2.463 ± 0.355 , $P < 0.001$ [Fig. 2E]). There were no significant effects of VGX-1027 on total or specific BAL fluid cell counts in PBS-instilled mice. Compared with PBS-pretreated PM_{2.5}-instilled mice, VGX-1027 significantly decreased total cell counts (316.250 ± 18.845 vs 486.875 ± 27.074 , $P < 0.01$, **Fig. 2A**); including macrophages (203.664 ± 9.644 vs 250.065 ± 13.457 , $P < 0.05$, **Fig. 2B**), lymphocytes (40.181 ± 2.952 vs 64.824 ± 4.127 , $P < 0.01$, **Fig. 2C**), neutrophils (62.030 ± 5.722 vs 174.827 ± 10.988 , $P < 0.05$, **Fig. 2D**) and eosinophils (6.625 ± 0.609 vs 9.659 ± 0.716 , $P < 0.01$, **Fig. 2E**) in BAL fluid.

3.3. BAL fluid cytokine levels and lung caspase-1 activity

PM_{2.5} intranasal instillation led to significant increases of cytokine levels in BAL fluid, including TNF- α (93.3 ± 12.7 vs 25.42 ± 9.6 pg/ml, $P < 0.001$, **Fig. 3A**), KC (184 ± 24 vs 43 ± 11 pg/ml, $P < 0.001$, **Fig. 3B**), IL-1 β (166 ± 15 vs 79 ± 12 pg/ml, $P < 0.05$, **Fig. 3C**), IL-6 (202 ± 21 vs 46 ± 9 pg/ml, $P < 0.05$, **Fig. 3D**) and IL-18 (66.6 ± 4.7 vs 44.3 ± 6.0 pg/ml, $P < 0.05$, **Fig. 3E**) compared to PBS-instilled mice. There were no changes in cytokine levels in VGX-1027-pretreated PBS-instilled mice compared with PBS-pretreated PBS-instilled mice. VGX-1027 pretreatment reduced PM_{2.5}-induced increases of TNF- α (36.2 ± 8.9 vs 93.3 ± 12.7 pg/ml, $P < 0.01$, **Fig. 3A**), KC (108 ± 18 vs 184 ± 24 pg/ml, $P < 0.05$, **Fig. 3B**), IL-1 β (110 ± 8 vs 166 ± 15 pg/ml, $P < 0.05$, **Fig. 3C**), IL-6 (66.2 ± 26.4 vs 202 ± 21 pg/ml, $P < 0.05$, **Fig. 3D**) and IL-18 (39.6 ± 3.0 vs 66.6 ± 4.7 pg/ml, $P < 0.01$, **Fig. 3E**) compared to PBS-pretreated PM_{2.5}-instilled mice .

Relative caspase-1 activity was significantly up-regulated in PBS-pretreated PM_{2.5}-instilled mice compared to PBS-pretreated PBS-instilled mice (113.3±5.5 vs 84.7±5.3 μM pNA, P<0.05) (**Fig. 3F**). VGX-1027 pretreatment did not affect lung relative caspase-1 activity in PBS-instilled mice compared with PBS-pretreated PBS-instilled mice. However, VGX-1027 pretreatment decreased lung relative caspase-1 activity in PM_{2.5}-instilled mice compared to PBS-pretreated PM_{2.5}-instilled mice (85.5±7.0 vs 113.3±5.5 μM pNA, P<0.05) (**Fig. 3F**).

3.4. Lung histopathological analysis

Representative images of lung tissue showing infiltration of inflammatory cells into the bronchial wall after instillation of PM_{2.5} are shown in **Figs. 4A-D**. PBS-pretreated PM_{2.5}-instilled mice had abundant inflammatory cells in their bronchial wall and alveolar septa compared with PBS-pretreated PBS-instilled mice (**Figs. 4A and 4C**) demonstrated by the increased inflammation scores (1.41±0.14 vs 0.24±0.04, P<0.001) (**Fig. 4E**). VGX-1027 treatment did not affect inflammation scores in control PBS-instilled mice. In contrast, VGX-1027 treatment decreased PM_{2.5}-induced lung inflammation scores compared with PBS-pretreated PM_{2.5}-instilled mice (0.65±0.06 vs 1.41±0.14, P<0.05) (**Fig. 4E**).

3.5. TLR4 expression in lung tissue

Immunohistochemistry staining showed that TLR4 expression was mainly distributed along the bronchial epithelium and in areas of inflammatory cell infiltration (**Figs. 5A-D**). TLR4 expression was increased in PBS-pretreated PM_{2.5}-instilled mice compared to PBS-pretreated PBS-instilled mice (P<0.01, **Fig. 5E**), as indicated by Western blot

analysis ($p < 0.05$, **Fig. 5F**). VGX-1027 treatment had no effect on TLR4 expression in control PBS-instilled mice. In contrast, there was a decrease in TLR4 immunostaining ($P < 0.05$, **Fig. 5E**) and expression ($P < 0.05$, **Fig. 5F**) in VGX-1027-pretreated PM_{2.5}-instilled mice compared to PBS-pretreated PM_{2.5}-instilled mice.

3.6. Western blot analysis in lung tissues

Protein levels of Mfn2 ($P < 0.01$, **Fig. 6A**) and OPA1 ($P < 0.05$, **Fig. 6B**) were decreased whilst those of MFF ($P < 0.01$, **Fig. 6C**) and Drp1 ($P < 0.05$, **Fig. 6D**) were increased in PBS-pretreated PM_{2.5}-instilled mice compared to PBS-pretreated PBS-instilled mice.

There were no significant effects of VGX-1027 on Mfn2, OPA1, MFF and Drp1 protein expression in PBS-instilled control mice. Pretreatment with VGX-1027 increased Mfn2 ($P < 0.05$, **Fig. 6A**), and OPA1 ($P < 0.05$, **Fig. 6B**) protein levels and decreased MFF ($P < 0.05$, **Fig. 6C**) protein levels in PM_{2.5}-instilled mice.

Compared to PBS-pretreated PBS-instilled mice, there was a significant increase in NF- κ B phosphorylation in PBS-pretreated PM_{2.5}-instilled mice ($P < 0.05$, **Fig. 6E**).

Pretreatment with VGX-1027 did not change the phosphorylation status of NF- κ B and p38 MAPK compared to PBS-pretreated PBS-instilled mice. Pretreatment with VGX-1027 inhibited the phosphorylation of NF- κ B ($P < 0.05$, **Fig. 6E**) and p38 MAPK ($P < 0.05$, **Fig. 6F**) in PM_{2.5}-instilled mice compared to PBS-pretreated PM_{2.5}-instilled mice.

PM_{2.5} instillation also enhanced the expression of NLRP3 ($P < 0.01$, **Fig. 6G**) and caspase-1 ($P < 0.05$, **Fig. 6H**) proteins compared to PBS-pretreated PBS-instilled mice.

Pretreatment with VGX-1027 did not affect NLRP3 and caspase-1 expression in PBS-instilled compared to PBS-pretreated PBS-instilled mice. VGX-1027-pretreated

PM_{2.5}-instilled mice demonstrated decreases in NLRP3 (P<0.01, **Fig. 6G**) and caspase-1 (P<0.05, **Fig. 6H**) expression compared to PBS-pretreated PM_{2.5}-instilled mice.

3.7. Cytokine mRNA levels and Caspase-1 activity in Beas-2b cells

PM_{2.5} stimulation (150 ng/ml) increased TNF- α (P<0.001, **Fig. 7A**), IL-1 β (P<0.001, **Fig. 7B**), IL-6 (P<0.001, **Fig. 7C**) and IL-18 mRNA levels (P<0.001, **Fig. 7D**) and increased relative caspase-1 activity (2.48 \pm 0.41 vs 1.07 \pm 0.18, P<0.05) (**Fig. 7E**) in Beas-2b cells after 24 h. VGX-1027 (50 μ M) pretreatment had no impact on cytokines mRNA expression and relative caspase-1 activity in vehicle-stimulated cells. Pretreatment with VGX-1027 for 1 h significantly inhibited PM_{2.5}-induced upregulation of TNF- α (P<0.001, **Fig. 7A**), IL-1 β (P<0.001, **Fig. 7B**), IL-6 (P<0.01, **Fig. 7C**) and IL-18 (P<0.05, **Fig. 7D**) mRNAs and the increase in relative caspase-1 activity (1.12 \pm 0.31 vs 2.48 \pm 0.41, P<0.05) (**Fig. 7E**) induced by PM_{2.5} in Beas-2b cells.

3.8. Western blot analysis of mitochondrial, inflammasome and inflammatory signaling pathways in Beas-2b cells

PM_{2.5} stimulation significantly reduced the protein expression of Mfn2 (P<0.01, **Fig. 8A**), and OPA1 (P<0.05, **Fig. 8B**) and increased that of MFF (P<0.05, **Fig. 8C**) and Drp1 (P<0.01, **Fig. 8D**) in Beas-2b cells after 24 h. There were no effects on the protein expression of Mfn2, OPA1, MFF and OPA1 after VGX-1027 pretreatment in vehicle-pretreated vehicle-stimulated cells. VGX-1027 promoted Mfn2 expression (P<0.05, **Fig. 8A**) and reduced MFF (P<0.05, **Fig. 8C**) and Drp1 (P<0.05, **Fig. 8D**) expression in PM_{2.5}-stimulated cells.

PM_{2.5} stimulation induced the activation of the TLR4 pathway as indicated by increased

TLR4 expression ($P < 0.05$, **Fig. 8E**), increased phosphorylation of NF- κ B ($P < 0.05$, **Fig. 8F**) and of p38 MAPK ($P < 0.05$, **Fig. 8G**) in Beas-2b cells after 24 h. VGX-1027 pretreatment did not affect TLR4 pathway in vehicle-stimulated group. VGX-1027 pretreatment inhibited TLR4 expression ($P < 0.05$, **Fig. 8E**) and decreased phosphorylation of NF- κ B ($P < 0.05$, **Fig. 8F**) and p38 MAPK ($P < 0.05$, **Fig. 8G**) in PM_{2.5}-stimulated Beas-2b cells after 24 h. Similarly, PM_{2.5} also enhanced NLRP3 ($P < 0.01$, **Fig. 8H**) and caspase-1 ($P < 0.05$, **Fig. 8I**) protein expression in Beas-2b cells after 24 h. There were no changes in NLRP3 and caspase-1 protein expression in VGX-1027-pretreated vehicle-stimulated cells compared to vehicle-pretreated vehicle-stimulated cells. VGX-1027 decreased the protein levels of both NLRP3 ($P < 0.05$, **Fig. 8H**) and caspase-1 ($P < 0.05$, **Fig. 8I**) in PM_{2.5}-stimulated cells.

4. Discussion

In the present study, we demonstrated that PM_{2.5} intranasal instillation for two consecutive days induced airway inflammation and BHR in mice. Pretreatment with VGX-1027, a TLR4 blocker, inhibited PM_{2.5}-induced airway inflammation and BHR. VGX-1027 inhibited the TLR4-NF- κ B-p38 MAPK pathway and the NLRP3-caspase-1 pathway *in vivo* and *in vitro*. Furthermore, VGX-1027 alleviated mitochondrial damage induced by PM_{2.5} by reversing the altered expression of fusion (Mfn2 and OPA1) and fission (MFF and Drp1) proteins both *in vivo* and *in vitro*. This data suggests that prophylactic treatment with VGX-1027 prevents PM_{2.5}-induced airway inflammation, BHR and mitochondrial damage through regulating the TLR4-NF- κ B-p38 MAPK and NLRP3-caspase-1 pathways and the expression of mitochondrial fusion/fission proteins.

PM_{2.5} exposure was associated with enhanced airway inflammation and immune cell infiltration as evidenced by increased macrophages, eosinophils, neutrophils and lymphocytes in lung tissues (Ogino et al., 2017; Wang et al., 2017; Wei and Tang, 2018). As the primary innate immune cell in the lung, alveolar macrophages phagocytose foreign particles and release proinflammatory cytokines including TNF- α , IL-1 β and IL-6 which, in turn, cause neutrophilic airway inflammation and even BHR (Strzelak et al., 2018; Wei and Tang, 2018). A recent study has indicated that intratracheal instillation of PM_{2.5} (7.8 mg/kg) caused inflammatory cell infiltration and proinflammatory cytokine production in mouse lung tissues (Jiang et al., 2017). Our results confirm and extend this data by highlighting the activation of several key pro-inflammatory processes such as the TLR4-NF- κ B-p38 MAPK, NLRP3-caspase-1 and mitochondrial fission/fusion pathways and linking these to BHR.

PM_{2.5} can initiate cell damage and inflammatory responses through interaction with TLRs (Wei and Tang, 2018), of which TLR4 is an important member. TLR4 activates NF- κ B and promotes cytokines production through an MyD88-dependent pathway (Chen et al., 2018). NF- κ B is a master transcription factor involved in both the innate and adaptive response (Miraghazadeh and Cook, 2018). In addition, TLR4 can also activate p38 MAPK and thereby drive the post-transcriptional regulation of inflammatory mediators such as TNF- α , IL-6 and IL-1 β (Singh et al., 2017). Several studies have demonstrated that PM_{2.5} activates TLR4-driven p38 MAPK/NF- κ B signaling pathways and induce the recruitment of inflammatory cells and the release of proinflammatory cytokines (He et al., 2017; Li et al., 2017; Song et al., 2017). Previous studies have also shown that treatment

with VGX-1027 inhibits the activation of the TLR4 signaling pathway (Cha et al., 2013; Laird et al., 2014). In our study, preventive treatment with VGX-1027 reduced the number of inflammatory cells and the levels of proinflammatory cytokines (TNF- α , KC, IL-1 β , IL-6 and IL-18) in BALF, attenuated inflammatory cell infiltration of lung tissues and decreased TNF- α , IL-1 β , IL-6 and IL-18 mRNA levels in Beas-2b cells. Moreover, both *in vivo* and *in vitro* studies showed that VGX-1027 inhibited the phosphorylation of both NF- κ B and p38 MAPK.

BHR is generally defined as the excessive contractile responses in bronchial smooth muscle exposed to a variety of inhaled stimuli (both chemical and physical) and, although it is not specific for asthma, it is considered as a hallmark of asthma (Borak and Lefkowitz, 2016). Transient and variable BHR may be derived mainly from the effects of acute lung inflammation (Cockcroft and Davis, 2006). Recent studies demonstrate that intranasal instillation of PM_{2.5} triggers BHR and allergic airway inflammation (Ogino et al., 2017; Ogino et al., 2014) and that increased BHR is closely related to neutrophilia and eosinophilia (McGovern et al., 2016; McGovern et al., 2015; Ogino et al., 2017). Indeed, organic dust-induced airway inflammation and BHR were significantly inhibited by neutrophil-depletion (McGovern et al., 2016) and bronchial smooth muscle contractility is modulated by cytokines such as TNF- α and IL-1 β (Deshpande et al., 2018; Sakai et al., 2017). TLR4 signaling may regulate BHR as deletion of TLR4 suppresses airway eosinophilia and BHR which was associated with a reduction in KC, IL-1 β , and TNF- α expression in a mouse model of allergic airway disease (Garantziotis and Hollingsworth, 2017; Thorburn et al., 2016). Hence, we speculate that VGX-1027 inhibited PM_{2.5}-induced

BHR by decreasing the levels of neutrophils, eosinophils and proinflammatory cytokines, as a result of inhibiting TLR4 signaling.

We report here that PM_{2.5} activates key inflammatory pathways in airway epithelial cells. Similar to TLRs, the NLRP3 inflammasome can act as a pattern recognition receptor (Sato and Kawakami, 2017) and phagocytosed PM_{2.5} can induce lysosomal rupture in epithelial cells which could, in turn, activate the NLRP3 inflammasome (Okada et al., 2014). Moreover, the damaged mitochondria observed following PM_{2.5} exposure in Beas-2b cells may release mitochondrial (mt)DNA which can also promote NLRP3 activation (Parker, 2018; Sandhir et al., 2017). Activated NLRP3 inflammasome accelerates the cleavage of pro-caspase-1 to activated caspase-1 which, in turn, cleaves pro-IL-1 β and pro-IL-18 into their mature forms (Poudel and Gurung, 2018; Prochnicki et al., 2016). Our results demonstrated that VGX-1027 inhibited PM_{2.5}-induced NLRP3 expression and caspase-1 activation which was associated with decreased the levels of both IL-1 β and IL-18 *in vivo* and *in vitro*. Further experiments are required to determine the specific roles of these cytokines in PM_{2.5}-induced airway inflammation and BHR.

PM_{2.5} exposure causes mitochondrial dysfunction and DNA damage in lung tissues and triggers a systemic inflammatory process (Guo et al., 2017; Li et al., 2015b; Zhang et al., 2018). In mammalian cells, mitochondrial structure is regulated by the fusion and fission process (Patrushev et al., 2015). Mitochondrial fusion is mainly driven by Mfn1/2 in the outer membrane and by OPA1 in the inner membrane (Szabo et al., 2018). A reduction in Mfn2 and OPA1 expression may produce pleiomorphic and enlarged mitochondria, increase mitochondrial permeability and trigger cell death (Ong et al., 2017;

Papanicolaou et al., 2011). Mitochondrial fission is mediated by Drp1, Fis1 and MFF, which induce fragmented discrete mitochondria. Activated cytoplasmic Drp1 translocates into mitochondria where it associates with MFF and Fis1 on the outer mitochondrial membrane to promote mitochondrial swelling and fragmentation (Ong et al., 2017; Zhao et al., 2017). Other studies in rat lungs have demonstrated that PM_{2.5} exposure down-regulates the expression of OPA1, Mfn1 and Mfn2, and promoted the expression of Drp1 and Fis1 which could disrupt the mitochondrial structural integrity and cause cell death (Guo et al., 2017; Li et al., 2015a; Li et al., 2015b). Consistent with previous studies, our *in vivo* study showed that VGX-1027 increased the expression of Mfn2 and OPA1 and reduced the expression of MFF. Our *in vitro* study showed that VGX-1027 promoted Mfn2 expression, and inhibited MFF and Drp1. Thus, VGX-1027 is capable of mitigating PM_{2.5}-induced mitochondrial damage and consolidating mitochondrial function. These results are similar to those seen with another TLR4 antagonist, TAK-242, which inhibited taurocholate-induced oxidative stress in mice pancreatic acinar cells by preventing the changes in expression of mitochondrial dynamic proteins (Pan et al., 2016).

In conclusion, our findings suggested that preventive treatment with VGX-1027 inhibited PM_{2.5}-induced airway inflammation, BHR and mitochondrial damage. These protective effects of VGX-1027 may be attributed to regulation of the TLR4-NF- κ B-p38 MAPK and NLRP3/Caspase-1 pathways and to restoration of mitochondrial function.

Acknowledgements

This work was supported by Action Plan for Science and Technology Innovation of

Shanghai Municipal Commission of Science and Technology (15140903400),
SMC-Chenxing Young Scholar Award Project from Shanghai Jiao Tong University, and
Natural Science Foundation of Anhui Province (KJ2018A0208).

Conflict of interest

The authors declare no conflict of interest.

Author Contributions Section

Conceptualization and Study Design: Yanbei Zhang, Feng li, Mengmeng Xu

Methodology: Mengmeng Xu, Feng Li, Muyun Wang, Lu Xu and Hai Zhang;

Statistical Analysis: Mengmeng Xu and Feng Li

Data Interpretation and Curation: Mengmeng Xu and Feng li

Manuscript Preparatio and Literature Search: Mengmeng Xu

Revise and Editing: Ian M Adcock, Kian Fan Chung, Feng Li, Mengmeng Xu and Yanbei Zhang;

Project Administration and Funding Acquisition: Yanbei Zhang and Feng Li.

References

Borak, J., Lefkowitz, R.Y., 2016. Bronchial hyperresponsiveness. *Occupational medicine* 66, 95-105.

Cha, J.J., Hyun, Y.Y., Lee, M.H., Kim, J.E., Nam, D.H., Song, H.K., Kang, Y.S., Lee, J.E.,

Kim, H.W., Han, J.Y., Cha, D.R., 2013. Renal protective effects of toll-like receptor 4 signaling blockade in type 2 diabetic mice. *Endocrinology* 154, 2144-2155.

Chen, C.Y., Kao, C.L., Liu, C.M., 2018. The Cancer Prevention, Anti-Inflammatory and Anti-Oxidation of Bioactive Phytochemicals Targeting the TLR4 Signaling Pathway.

International journal of molecular sciences 19.

Cockcroft, D.W., Davis, B.E., 2006. Mechanisms of airway hyperresponsiveness. The Journal of allergy and clinical immunology 118, 551-559; quiz 560-551.

Deshpande, D.A., Guedes, A.G.P., Graeff, R., Dogan, S., Subramanian, S., Walseth, T.F., Kannan, M.S., 2018. CD38/cADPR Signaling Pathway in Airway Disease: Regulatory Mechanisms. Mediators of inflammation 2018, 8942042.

Fagone, P., Muthumani, K., Mangano, K., Magro, G., Meroni, P.L., Kim, J.J., Sardesai, N.Y., Weiner, D.B., Nicoletti, F., 2014. VGX-1027 modulates genes involved in lipopolysaccharide-induced Toll-like receptor 4 activation and in a murine model of systemic lupus erythematosus. Immunology 142, 594-602.

Garantziotis, S., Hollingsworth, J.W., 2017. Comment on Expression of Concern: TLR4 Is Necessary for Hyaluronan-mediated Airway Hyperresponsiveness after Ozone Inhalation. American journal of respiratory and critical care medicine 196, 249-250.

Guo, Z., Hong, Z., Dong, W., Deng, C., Zhao, R., Xu, J., Zhuang, G., Zhang, R., 2017. PM2.5-Induced Oxidative Stress and Mitochondrial Damage in the Nasal Mucosa of Rats. International journal of environmental research and public health 14.

He, M., Ichinose, T., Yoshida, Y., Arashidani, K., Yoshida, S., Takano, H., Sun, G., Shibamoto, T., 2017. Urban PM2.5 exacerbates allergic inflammation in the murine lung via a TLR2/TLR4/MyD88-signaling pathway. Scientific reports 7, 11027.

Jiang, S., Bo, L., Du, X., Liu, J., Zeng, X., He, G., Sun, Q., Kan, H., Song, W., Xie, Y.,

Zhao, J., 2017. CARD9-mediated ambient PM_{2.5}-induced pulmonary injury is associated with Th17 cell. *Toxicology letters* 273, 36-43.

Kawasaki, T., Kawai, T., 2014. Toll-like receptor signaling pathways. *Frontiers in immunology* 5, 461.

Laird, M.D., Shields, J.S., Sukumari-Ramesh, S., Kimbler, D.E., Fessler, R.D., Shakir, B., Youssef, P., Yanasak, N., Vender, J.R., Dhandapani, K.M., 2014. High mobility group box protein-1 promotes cerebral edema after traumatic brain injury via activation of toll-like receptor 4. *Glia* 62, 26-38.

Li, F., Wiegman, C., Seiffert, J.M., Zhu, J., Clarke, C., Chang, Y., Bhavsar, P., Adcock, I., Zhang, J., Zhou, X., Chung, K.F., 2013. Effects of N-acetylcysteine in ozone-induced chronic obstructive pulmonary disease model. *PloS one* 8, e80782.

Li, R., Kou, X., Geng, H., Xie, J., Tian, J., Cai, Z., Dong, C., 2015a. Mitochondrial damage: an important mechanism of ambient PM_{2.5} exposure-induced acute heart injury in rats. *Journal of hazardous materials* 287, 392-401.

Li, R., Kou, X., Geng, H., Xie, J., Yang, Z., Zhang, Y., Cai, Z., Dong, C., 2015b. Effect of ambient PM_{2.5} on lung mitochondrial damage and fusion/fission gene expression in rats. *Chemical research in toxicology* 28, 408-418.

Li, R., Zhao, L., Tong, J., Yan, Y., Xu, C., 2017. Fine Particulate Matter and Sulfur Dioxide Coexposures Induce Rat Lung Pathological Injury and Inflammatory Responses Via TLR4/p38/NF-kappaB Pathway. *International journal of toxicology* 36, 165-173.

Lin, Y., Zou, J., Yang, W., Li, C.Q., 2018. A Review of Recent Advances in Research on PM_{2.5} in China. *International journal of environmental research and public health* 15.

McGovern, T.K., Chen, M., Allard, B., Larsson, K., Martin, J.G., Adner, M., 2016.

Neutrophilic oxidative stress mediates organic dust-induced pulmonary inflammation and airway hyperresponsiveness. *American journal of physiology. Lung cellular and molecular physiology* 310, L155-165.

McGovern, T.K., Goldberger, M., Allard, B., Farahnak, S., Hamamoto, Y., O'Sullivan, M., Hirota, N., Martel, G., Rousseau, S., Martin, J.G., 2015. Neutrophils mediate airway hyperresponsiveness after chlorine-induced airway injury in the mouse. *American journal of respiratory cell and molecular biology* 52, 513-522.

Miraghadzadeh, B., Cook, M.C., 2018. Nuclear Factor-kappaB in Autoimmunity: Man and Mouse. *Frontiers in immunology* 9, 613.

Miyata, R., van Eeden, S.F., 2011. The innate and adaptive immune response induced by alveolar macrophages exposed to ambient particulate matter. *Toxicology and applied pharmacology* 257, 209-226.

Ogino, K., Nagaoka, K., Okuda, T., Oka, A., Kubo, M., Eguchi, E., Fujikura, Y., 2017. PM2.5-induced airway inflammation and hyperresponsiveness in NC/Nga mice. *Environmental toxicology* 32, 1047-1054.

Ogino, K., Zhang, R., Takahashi, H., Takemoto, K., Kubo, M., Murakami, I., Wang, D.H., Fujikura, Y., 2014. Allergic airway inflammation by nasal inoculation of particulate matter (PM2.5) in NC/Nga mice. *PloS one* 9, e92710.

Okada, M., Matsuzawa, A., Yoshimura, A., Ichijo, H., 2014. The lysosome rupture-activated TAK1-JNK pathway regulates NLRP3 inflammasome activation. *The Journal of biological chemistry* 289, 32926-32936.

- Ong, S.B., Kalkhoran, S.B., Hernandez-Resendiz, S., Samangouei, P., Ong, S.G., Hausenloy, D.J., 2017. Mitochondrial-Shaping Proteins in Cardiac Health and Disease - the Long and the Short of It! *Cardiovascular drugs and therapy* 31, 87-107.
- Ovrevik, J., Refsnes, M., Lag, M., Holme, J.A., Schwarze, P.E., 2015. Activation of Proinflammatory Responses in Cells of the Airway Mucosa by Particulate Matter: Oxidant- and Non-Oxidant-Mediated Triggering Mechanisms. *Biomolecules* 5, 1399-1440.
- Pan, L.F., Yu, L., Wang, L.M., He, J.T., Sun, J.L., Wang, X.B., Bai, Z.H., Su, L.J., Pei, H.H., 2016. The toll-like receptor 4 antagonist transforming growth factor-beta-activated kinase(TAK)-242 attenuates taurocholate-induced oxidative stress through regulating mitochondrial function in mice pancreatic acinar cells. *The Journal of surgical research* 206, 298-306.
- Papanicolaou, K.N., Khairallah, R.J., Ngoh, G.A., Chikando, A., Luptak, I., O'Shea, K.M., Riley, D.D., Lugas, J.J., Colucci, W.S., Lederer, W.J., Stanley, W.C., Walsh, K., 2011. Mitofusin-2 maintains mitochondrial structure and contributes to stress-induced permeability transition in cardiac myocytes. *Molecular and cellular biology* 31, 1309-1328.
- Parker, J.C., 2018. Mitochondrial damage pathways in ventilator induced lung injury (VILI): an update. *Journal of lung health and diseases* 2, 18-22.
- Patrushev, M.V., Mazunin, I.O., Vinogradova, E.N., Kamenski, P.A., 2015. Mitochondrial Fission and Fusion. *Biochemistry. Biokhimiia* 80, 1457-1464.
- Poudel, B., Gurung, P., 2018. An update on cell intrinsic negative regulators of the NLRP3 inflammasome. *Journal of leukocyte biology*.
- Prochnicki, T., Mangan, M.S., Latz, E., 2016. Recent insights into the molecular

mechanisms of the NLRP3 inflammasome activation. *F1000Research* 5.

Sakai, H., Suto, W., Kai, Y., Chiba, Y., 2017. Mechanisms underlying the pathogenesis of hyper-contractility of bronchial smooth muscle in allergic asthma. *Journal of smooth muscle research = Nihon Heikatsukin Gakkai kikanshi* 53, 37-47.

Sandhir, R., Halder, A., Sunkaria, A., 2017. Mitochondria as a centrally positioned hub in the innate immune response. *Biochimica et biophysica acta* 1863, 1090-1097.

Sato, K., Kawakami, K., 2017. Recognition of *Cryptococcus neoformans* by Pattern Recognition Receptors and its Role in Host Defense to This Infection. *Medical mycology journal* 58, J83-J90.

Singh, R.K., Najmi, A.K., Dastidar, S.G., 2017. Biological functions and role of mitogen-activated protein kinase activated protein kinase 2 (MK2) in inflammatory diseases. *Pharmacological reports : PR* 69, 746-756.

Song, L., Li, D., Li, X., Ma, L., Bai, X., Wen, Z., Zhang, X., Chen, D., Peng, L., 2017.

Exposure to PM_{2.5} induces aberrant activation of NF- κ B in human airway epithelial cells by downregulating miR-331 expression. *Environ Toxicol Pharmacol* 50, 192-199.

Stojanovic, I., Cuzzocrea, S., Mangano, K., Mazzon, E., Miljkovic, D., Wang, M., Donia, M., Al Abed, Y., Kim, J., Nicoletti, F., Stosic-Grujicic, S., Claesson, M., 2007. In vitro, ex vivo and in vivo immunopharmacological activities of the isoxazoline compound

VGX-1027: modulation of cytokine synthesis and prevention of both organ-specific and systemic autoimmune diseases in murine models. *Clinical immunology* 123, 311-323.

Strzelak, A., Ratajczak, A., Adamiec, A., Feleszko, W., 2018. Tobacco Smoke Induces and Alters Immune Responses in the Lung Triggering Inflammation, Allergy, Asthma and Other

Lung Diseases: A Mechanistic Review. *International journal of environmental research and public health* 15.

Szabo, A., Sumegi, K., Fekete, K., Hocsak, E., Debreceni, B., Setalo, G., Jr., Kovacs, K., Deres, L., Kengyel, A., Kovacs, D., Mandl, J., Nyitrai, M., Febbraio, M.A., Gallyas, F., Jr., Sumegi, B., 2018. Activation of mitochondrial fusion provides a new treatment for mitochondria-related diseases. *Biochemical pharmacology* 150, 86-96.

Thorburn, A.N., Tseng, H.Y., Donovan, C., Hansbro, N.G., Jarnicki, A.G., Foster, P.S., Gibson, P.G., Hansbro, P.M., 2016. TLR2, TLR4 AND MyD88 Mediate Allergic Airway Disease (AAD) and *Streptococcus pneumoniae*-Induced Suppression of AAD. *PloS one* 11, e0156402.

Wang, H., Song, L., Ju, W., Wang, X., Dong, L., Zhang, Y., Ya, P., Yang, C., Li, F., 2017. The acute airway inflammation induced by PM2.5 exposure and the treatment of essential oils in Balb/c mice. *Scientific reports* 7, 44256.

Wei, T., Tang, M., 2018. Biological effects of airborne fine particulate matter (PM2.5) exposure on pulmonary immune system. *Environ Toxicol Pharmacol* 60, 195-201.

Xing, Y.F., Xu, Y.H., Shi, M.H., Lian, Y.X., 2016. The impact of PM2.5 on the human respiratory system. *Journal of thoracic disease* 8, E69-74.

Zhang, J., Liu, J., Ren, L., Wei, J., Duan, J., Zhang, L., Zhou, X., Sun, Z., 2018. PM2.5 induces male reproductive toxicity via mitochondrial dysfunction, DNA damage and RIPK1 mediated apoptotic signaling pathway. *The Science of the total environment* 634, 1435-1444.

Zhao, Y., Ponnusamy, M., Dong, Y., Zhang, L., Wang, K., Li, P., 2017. Effects of miRNAs

on myocardial apoptosis by modulating mitochondria related proteins. Clinical and experimental pharmacology & physiology 44, 431-440.

Fig. 1. Effect of PM_{2.5} (7.8 mg/kg) exposure and of VGX-1027 (25 mg/kg) pretreatment on lung function. Mean percentage increase in lung resistance (R_L) to increasing concentrations of acetylcholine (ACh) (A). * P<0.05, ** P<0.01, and *** P<0.001 compared with the PBS-pretreated PBS-instilled mice. &&P<0.01, and &&&P <0.001 compared with the VGX-1027-pretreated PBS-instilled mice. ##P<0.01 and ###P<0.01 compared with the VGX-1027-pretreated PM_{2.5}-instilled mice (A). Individual and mean airway resistance at 256 mg/mL ACh (B). -logPC₂₀₀ was measured as an indicator of bronchial responsiveness. Individual and mean -logPC₂₀₀ (C). * P<0.05, ** P<0.01, *** P<0.001 compared with PBS-pretreated PM_{2.5}-instilled mice.

Fig. 2. Effect of PM_{2.5} (7.8 mg/kg) exposure and of VGX-1027 (25 mg/kg) pretreatment on inflammation. Individual and mean numbers of total cells (TOTAL) (A), macrophages (MAC) (B), lymphocytes (LYM) (C), neutrophils (NEU) (D), and eosinophils (EOS) (E) in bronchoalveolar lavage (BAL) fluid. * P<0.05, ** P<0.01, *** P<0.001 compared with PBS-pretreated PM_{2.5}-instilled mice.

Fig. 3. Effect of PM_{2.5} (7.8 mg/kg) exposure and of VGX-1027 (25 mg/kg) pretreatment on individual and mean levels of TNF- α (A), chemokine (C-X-C motif) ligand 1 (KC) (B), IL-1 β (C), IL-6 (D) and IL-18 (E) in bronchoalveolar lavage (BAL) fluid. Individual and mean relative caspase-1 activity in lung tissue homogenates (F). * P<0.05, ** P<0.01, *** P<0.001 compared with PBS-pretreated PM_{2.5}-instilled mice.

Fig. 4. Effect of PM_{2.5} (7.8 mg/kg) exposure and of VGX-1027 (25 mg/kg) pretreatment on lung inflammation. Representative bronchial photomicrographs of mouse lung tissues in hematoxylin

and eosin-stained sections from PBS-pretreated PBS-instilled mice (A), VGX-1027-pretreated PBS-instilled mice (B), PBS-pretreated PM_{2.5}-instilled mice (C), and VGX-1027-pretreated PM_{2.5}-instilled mice (D), bar 100µm. Individual and mean values of inflammation scores measured from H&E-stained sections (E). * P<0.05, ** P<0.01, *** P<0.001 compared with PBS-pretreated PM_{2.5}-instilled mice. Arrows indicate inflamed airways and alveolar septa.

Fig. 5. Effect of PM_{2.5} (7.8 mg/kg) exposure and of VGX-1027 (25 mg/kg) pretreatment on lung TLR4 expression. Immunohistochemical analysis of TLR4 expression (brown staining, arrowed) in mouse lung tissue sections in PBS-pretreated PBS-instilled mice (A), VGX-1027-pretreated PBS-instilled mice (B), PBS-pretreated PM_{2.5}-instilled mice (C), and VGX-1027-pretreated PM_{2.5}-instilled mice (D) (original magnification ×100). Individual and mean immunostaining scores of TLR4 measured in immunohistochemical sections (E). Western blot analysis of the expression of TLR4 compared to β-actin in mouse lung tissue homogenates (F). * P<0.05, ** P<0.01, *** P<0.001 compared with PBS-pretreated PM_{2.5}-instilled mice.

Fig. 6. The effect of PM_{2.5} (7.8 mg/kg) exposure and of VGX-1027 (25 mg/kg) pretreatment on the relative protein expression of Mitofusin 2 (Mfn2) (A), Optic Atrophy 1 (OPA1) (B), Mitochondrial fission factor (MFF) (C) and Dynamin-related protein 1 (Drp1) (D) to glyceraldehyde-3-phosphate dehydrogenase (GAPDH) in mouse lung tissue homogenates. The ratio of phosphorylated (phospho) NF-κB to total NF-κB (E), phosphorylated (phospho) p38 MAPK to total p38 MAPK (F) is also shown as is the relative expression of Nod-like receptor pyrin domain containing 3 (NLRP3) (G) and Caspase-1 (H) compared to GAPDH. Each panel shows a representative Western blot.

* P<0.05, ** P<0.01, *** P<0.001 compared with PBS-pretreated PM_{2.5}-instilled mice.

Fig. 7. The effect of PM_{2.5} (150 ng/ml) exposure and of VGX-1027 (50 µM) pretreatment on

inflammatory mediator mRNA expression and on caspase-1 activity after 24 h. Quantitative RT-PCR measurement of the individual and mean relative mRNA levels of TNF- α (A), IL-1 β (B), IL-6 (C) and IL-18 (D) in Beas-2b cells. Relative and mean caspase-1 activity in Beas-2b cells (E).

*P<0.05, **P<0.01, ***P<0.001 compared with the PM_{2.5} stimulated cells.

Fig. 8. The effect of PM_{2.5} (150 ng/ml) exposure and of VGX-1027 (50 μ M) pretreatment on mitochondrial proteins, inflammasome and inflammatory signaling pathways after 24 h. Western blot analysis of the relative protein expression of Mitofusin 2 (Mfn2, A), Optic Atrophy 1 (OPA1, B), Mitochondrial fission factor (MFF, C), Dynamin-related protein 1 (Drp1, D), Toll-like receptor 4 (TLR4, E), Nod-like receptor pyrin domain containing 3 (NLRP3, H) and caspase-1 (I) to glyceraldehyde-3-phosphate dehydrogenase (GAPDH) or β -actin. The ratio of phosphorylated (phospho) nuclear factor κ B (NF- κ B) to total NF- κ B (F) and of phosphorylated (phospho) p38 mitogen activated protein kinase (MAPK) to total p38 MAPK (G) in Beas-2b cells is also shown. Each panel shows a representative Western blot. *P<0.05, **P<0.01, ***P<0.001 compared with PM_{2.5} stimulated cells.

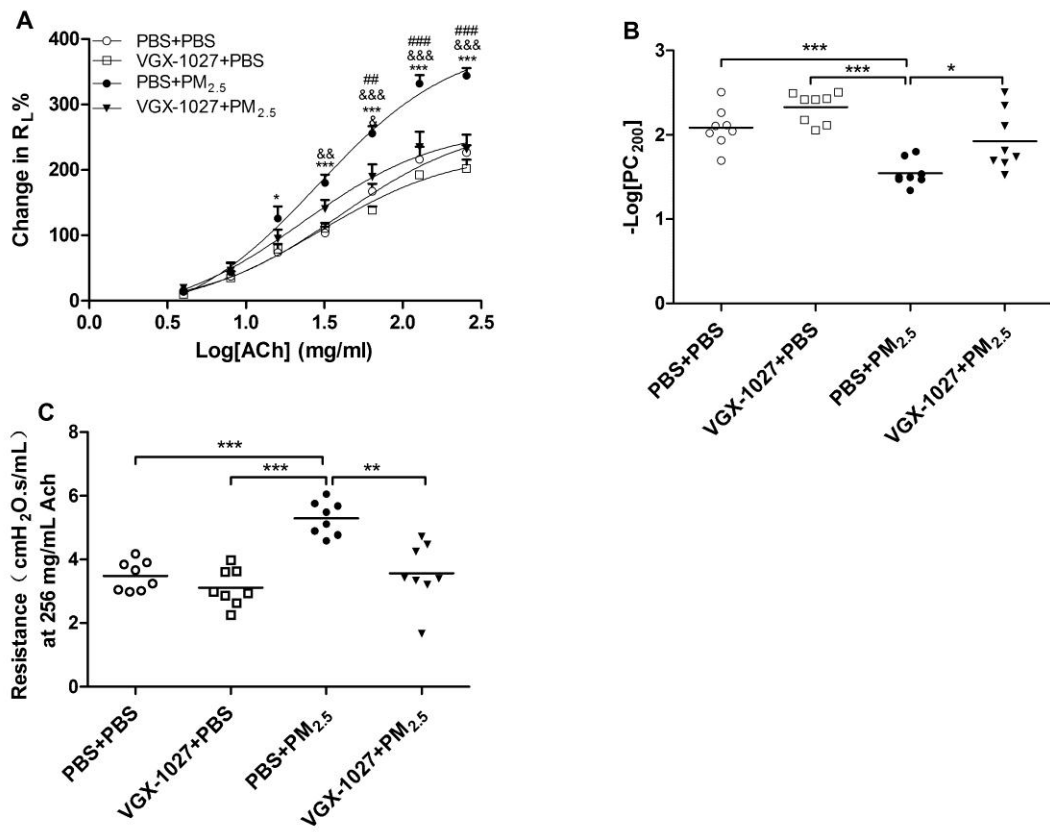


Fig. 1

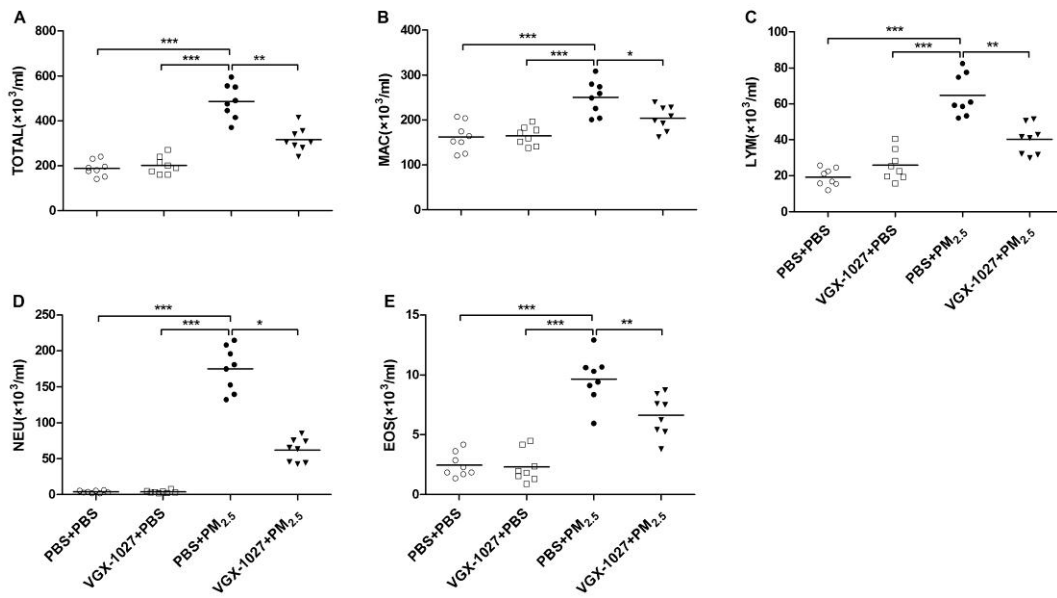


Fig. 2

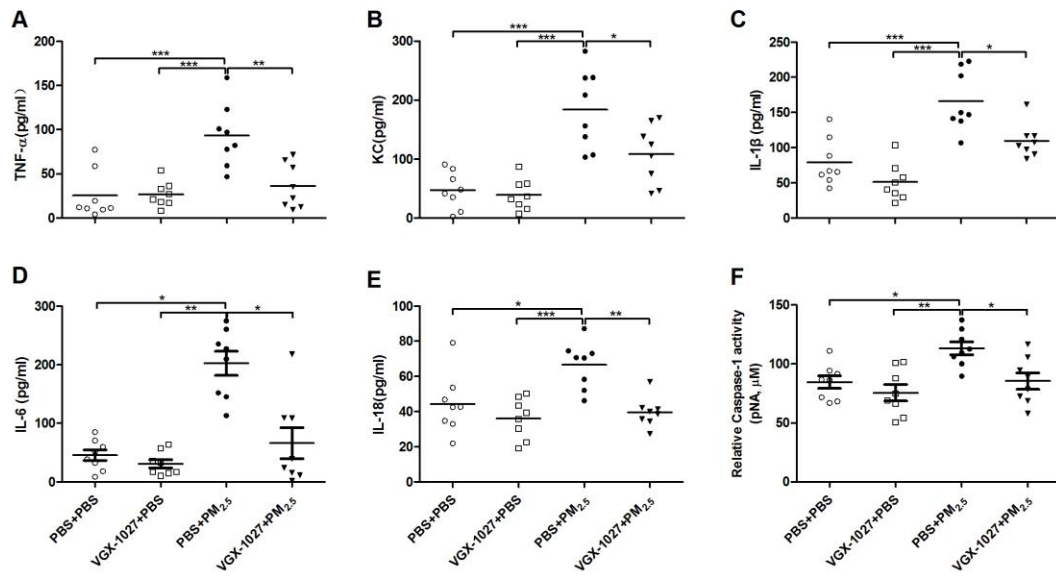


Fig. 3

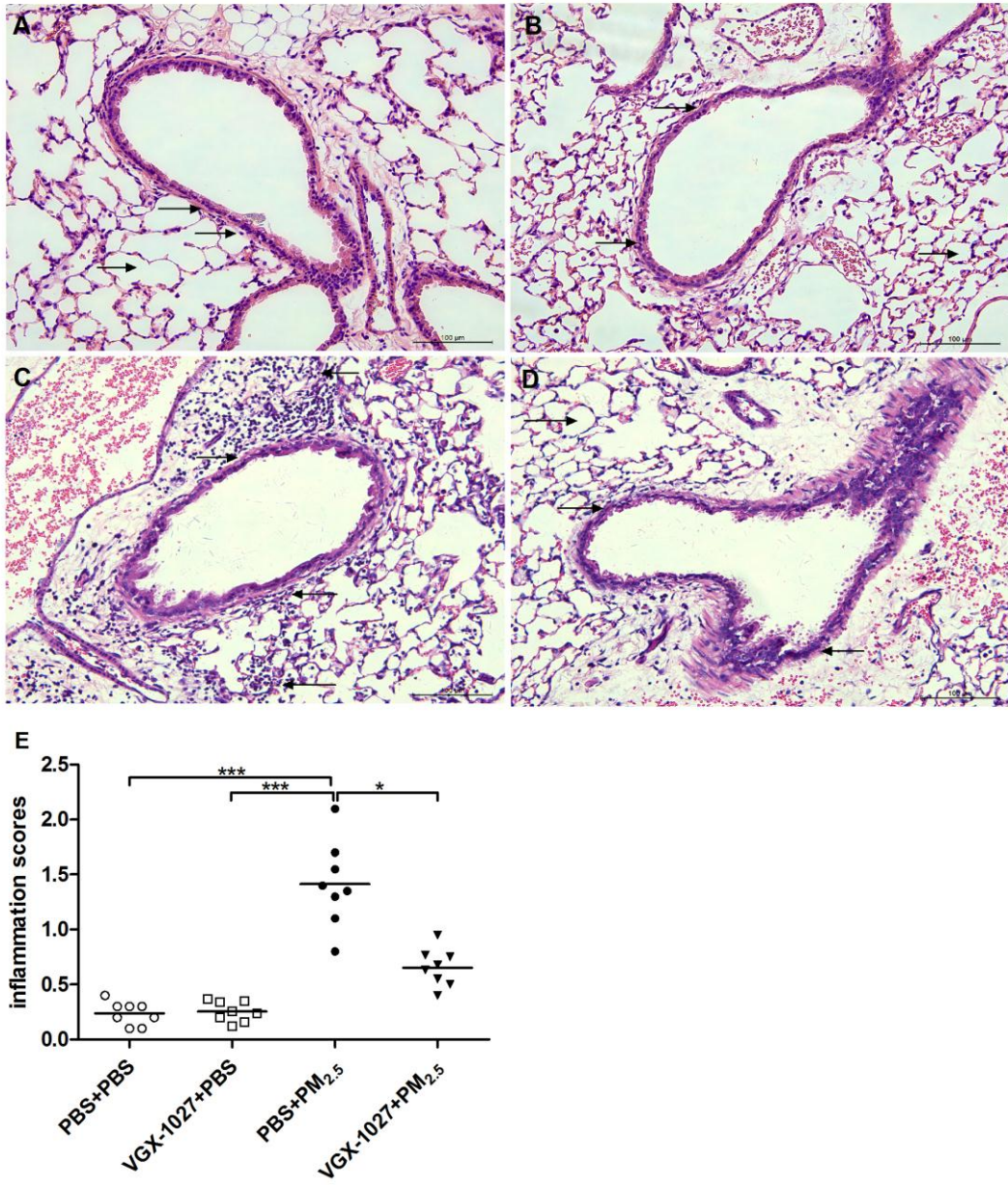


Fig. 4

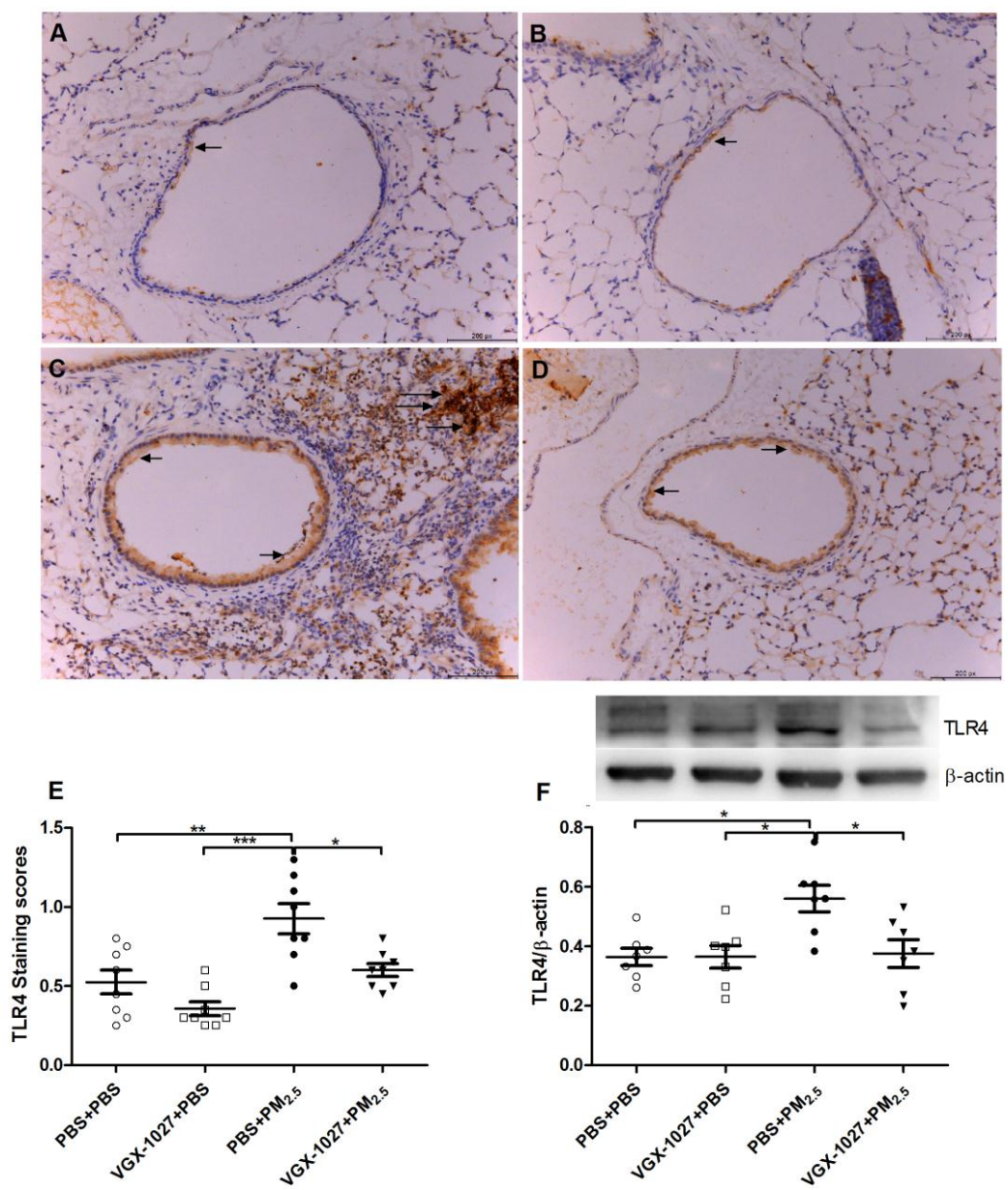


Fig. 5

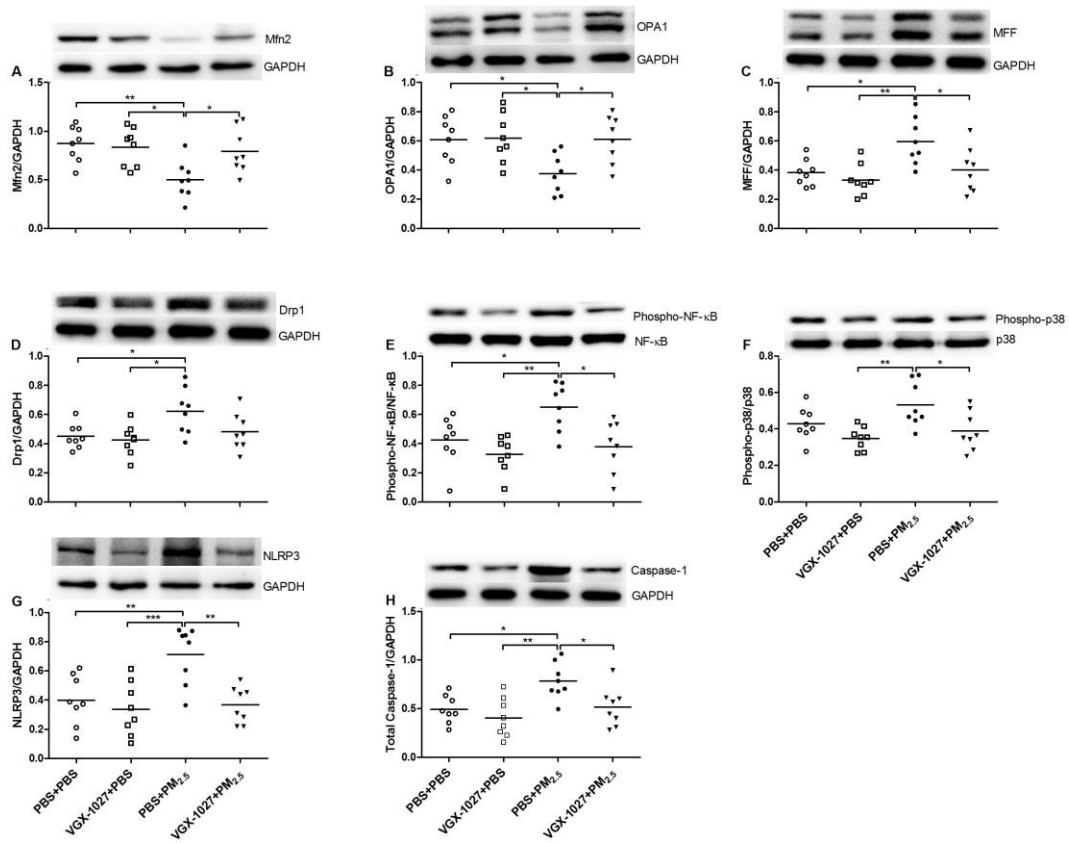


Fig. 6

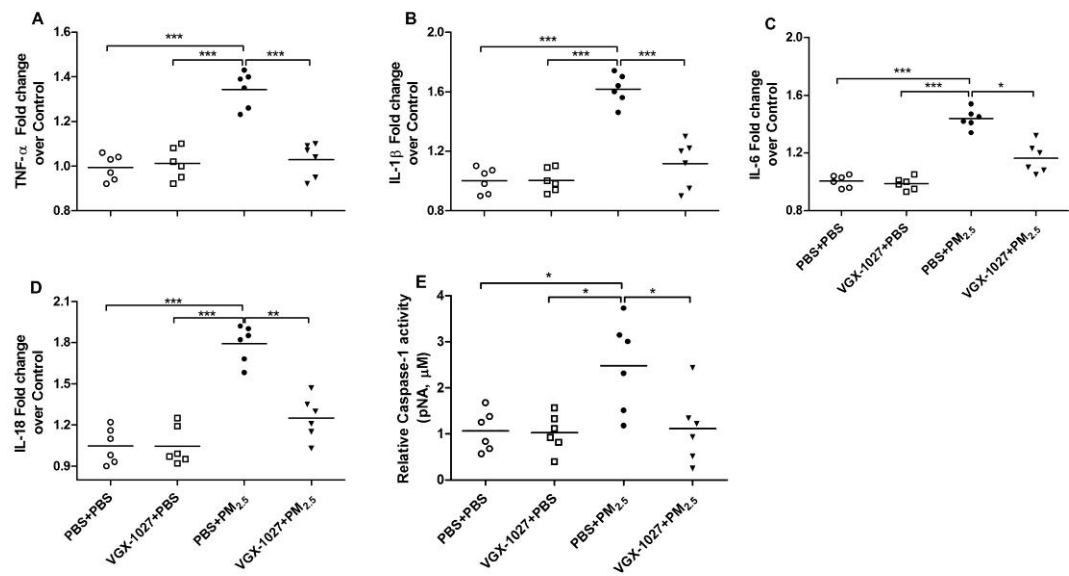


Fig. 7

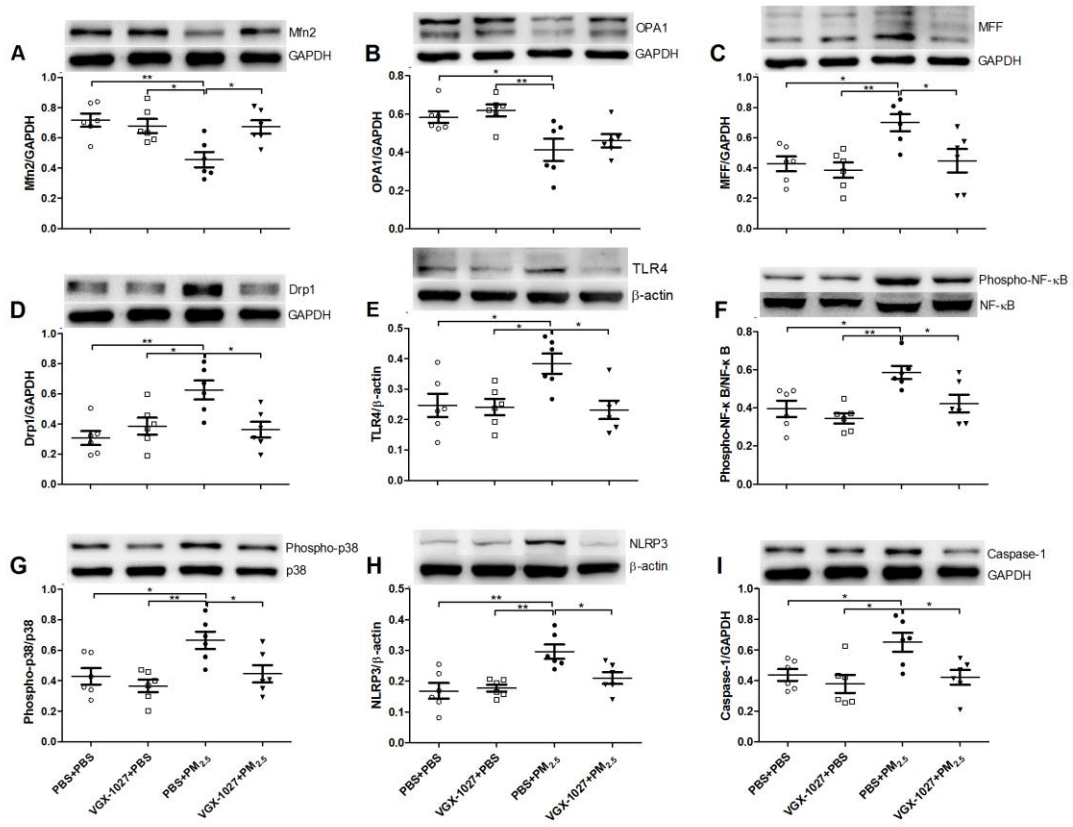


Fig. 8